

Contents

Abbott, M.J., → Stolz, A.J., et al. 374–389
Aksyuk, A.M., → Bruckmann-Benke, P., et al. 91–96
Andersen, T., → Neumann, E.-R., et al. 184–193
Bacon, C.R., Druitt, T.H.: Compositional evolution of the zoned calc-alkaline magma chamber of Mount Mazama, Crater Lake, Oregon 224–256
Barsczus, H.G., → Dupuy, C., et al. 293–302
Baumgartner, L.P., Rumble III, D.: Transport of stable isotopes: I.: Development of a kinetic continuum theory for stable isotope transport 417–430
Boivin, P., → Liotard, J.M., et al. 81–90
Briot, D., → Liotard, J.M., et al. 81–90
Brown, W.L., Parsons, I.: Zoned ternary feldspars in the Klokken intrusion: exsolution microtextures and mechanisms 444–454
Brown, W.L., → Parsons, I. 431–443
Bruckmann-Benke, P., Chatterjee, N.D., Aksyuk, A.M.: Thermodynamic properties of $Zn(Al, Cr)_2O_4$ spinels at high temperatures and pressures 91–96
Chatterjee, N.D., → Bruckmann-Benke, P., et al. 91–96
Chipera, S.J., Perkins, D.: Evaluation of biotite-garnet geothermometers: application to the English River subprovince, Ontario 40–48
Cohen, A.S., O'Nions, R.K., Siegenthaler, R., Griffin, W.L.: Chronology of the pressure-temperature history recorded by a granulite terrain 303–311
Corfu, F.: Differential response of U–Pb systems in coexisting accessory minerals, Winnipeg River Subprovince, Canadian Shield: implications for Archean crustal growth and stabilization 312–325
Cuney, M., → Turpin, L., et al. 139–147
Dostal, J., → Dupuy, C., et al. 293–302
Druitt, T.H., → Bacon, C.R. 224–256
Dunning, G.R., Pedersen, R.B.: U/Pb ages of ophiolites and arc-related plutons of the Norwegian Caledonides: implications for the development of Iapetus 13–23
Dupuy, C., Barsczus, H.G., Liotard, J.M., Dostal, J.: Trace element evidence for the origin of ocean island basalts: an example from the Austral Islands (French Polynesia) 293–302
Ellam, R.M., Hawkesworth, C.J.: Elemental and isotopic variations in subduction related basalts: evidence for a three component model 72–80
Essene, E.J., → Sharp, Z.D., et al. 490–501
Faul, H., → Lutz, T.M., et al. 212–223
Ferry, J.M.: Contrasting mechanisms of fluid flow through adjacent stratigraphic units during regional metamorphism, south-central Maine, USA 1–12
Foden, J.D., → Stolz, A.J., et al. 374–389
Foland, K.A., Raczek, I., Henderson, C.M.B., Hofmann, A.W.: Petrogenesis of the magmatic complex at Mount Ascutney, Vermont, USA. II. Contamination of mafic magmas and country rock model ages based upon Nd isotopes 408–416
Foland, K.A., → Lutz, T.M., et al. 212–223
Fourcade, S., → Ouzegane, K., et al. 277–292
Ghent, E.D.: Tremolite and H_2O activity attending metamorphism of hornblende-plagioclase-garnet assemblages 163–168
Grant, S.M.: Diffusion models for corona formation in metagabbros from the Western Grenville Province, Canada 49–63
Griffin, W.L., → Cohen, A.S., et al. 303–311
Hawkesworth, C.J., → Ellam, R.M. 72–80
Henderson, C.M.B., → Foland, K.A., et al. 408–416
Henry, C.D., Price, J.G., Smyth, R.C.: Chemical and thermal zonation in a mildly alkaline magma system Infiernito Caldera, Trans-Pecos, Texas 194–211
Hensel, H.D., → Wilkinson, J.F.G. 326–345
Hildreth, W., Moorbath, S.: Crustal contributions to arc magmatism in the Andes of Central Chile 455–489
Hofmann, A.W., → Foland, K.A., et al. 408–416
Hofmann, A.W., → Liew, T.C. 129–138
Holloway, J.R., → Vielzeuf, D. 257–276
James, D., → Maaløe, S., et al. 401–407
Javoy, M., → Ouzegane, K., et al. 277–292
Johnston, A.D., Wyllie, P.J.: Interaction of granitic and basic magmas: experimental observations on contamination processes at 10 kbar with H_2O 352–362
Kienast, J.-R., → Ouzegane, K., et al. 277–292
Kreulen, R.: High integrated fluid/rock ratios during metamorphism at Naxos: evidence from carbon isotopes of calcite in schists and fluid inclusions 28–32
Liew, T.C., Hofmann, A.W.: Precambrian crustal components, plutonic associations, plate environment of the Hercynian Fold Belt of central Europe: Indications from a Nd and Sr isotopic study 129–138
Liotard, J.M., Briot, D., Boivin, P.: Petrological and geochemical relationships between pyroxene megacrysts and associated alkali-basalts from Massif Central (France) 81–90
Liotard, J.M., → Dupuy, C., et al. 293–302
Lonker, S.W.: An occurrence of grandidierite, kornerupine, and tourmaline in southeastern Ontario, Canada 502–516
Lutz, T.M., Foland, K.A., Faul, H., Srogi, L.A.: The strontium and oxygen isotopic record of hydrothermal alteration of syenites from the Abu Khrug complex, Egypt 212–223
Maaløe, S., Pedersen, R.B., James, D.: Delayed fractionation of basaltic lavas 401–407
Maruejol, P., → Turpin, L., et al. 139–147
Matioli, G.S., Wood, B.J.: Magnetite activities across the $MgAl_2O_4$ – Fe_2O_3 spinel join, with application to thermobarometric estimates of upper mantle oxygen fugacity 148–162
Mearns, E.W., → Neumann, E.-R., et al. 184–193
Medhioub, M., → Velde, B. 122–127
Menute, J.F.: The petrogenesis of massif anorthosites: a Nd and Sr isotopic investigation of the Proterozoic of Rogaland/Vest-Agder, SW Norway 363–373
Moorbath, S., → Hildreth, W. 455–489
Morrison, J., Valley, J.: Contamination of the Marcy Anorthosite Massif, Adirondack Mountains, NY: petrologic and isotopic evidence 97–108
Neumann, E.-R., Andersen, T., Mearns, E.W.: Olivine clinopyroxenite xenoliths in the Oslo Rift, SE Norway 184–193
O'Neil, J.R., → Sharp, Z.D., et al. 490–501
O'Nions, R.K., → Cohen, A.S., et al. 303–311
Ouzegane, K., Fourcade, S., Kienast, J.-R., Javoy, M.: New carbonatite complexes in the Archaean in'Ouzzal nucleus (Ahaggar, Algeria): mineralogical and geochemical data 277–292
Parsons, I., Brown, W.L.: Sidewall crystallization in the Klokken intrusion: zoned ternary feldspars and coexisting minerals 431–443
Parsons, I., → Brown, W.L. 444–454
Pedersen, R.B., → Dunning, G.R. 13–23
Pedersen, R.B., → Maaløe, S., et al. 401–407
Perkins, D., → Chipera, S.J. 40–48
Powell, R., Sandford, M.: Sapphirine and spinel phase relationships in the system FeO – MgO – Al_2O_3 – SiO_2 – TiO_2 – O_2 in the presence of quartz and hypersthene 64–71
Price, J.G., → Henry, C.D., et al. 194–211
Puhan, D.: Reverse age relations of talc and tremolite deduced from reaction textures in metamorphosed siliceous dolomites of the southern Damara Orogen (Namibia) 24–27
Raczek, I., → Foland, K.A., et al. 408–416
Rumble III, D., → Baumgartner, L.P. 417–430
Sanders, I.S.: Plagioclase breakdown and regeneration reactions in Grenville kyanite eclogite at Glenelg, NW Scotland 33–39

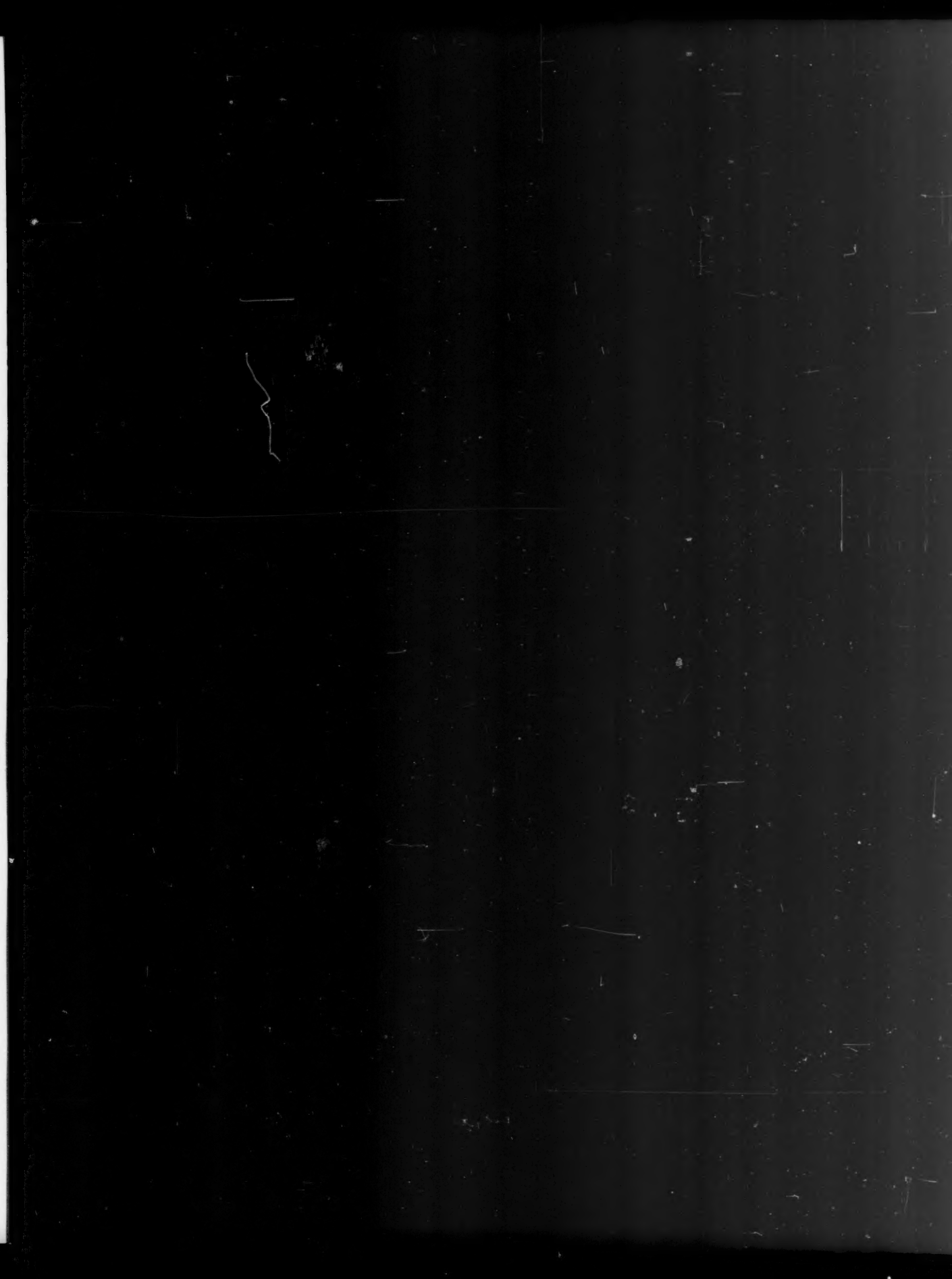
Sandiford, M., → Powell, R. 64-71
Sharp, Z.D., O'Neil, J.R., Essene, E.J.: Oxygen isotope variations in granulite-grade iron formations: constraints on oxygen diffusion and retrograde isotopic exchange 490-501
Siegenthaler, R., → Cohen, A.S., et al. 303-311
Sinha, A.K., → Wayne, D.M. 109-121
Smyth, R.C., → Henry, C.D., et al. 194-211
Spear, F.S.: Thermodynamic projection and extrapolation of high-variance mineral assemblages 346-351
Srogi, L.A., → Lutz, T.M., et al. 212-223
Stolz, A.J., Varne, R., Wheller, G.E., Foden, J.D., Abbott, M.J.: The geochemistry and petrogenesis of K-rich alkaline volcanics from the Batu Tara volcano, eastern Sunda arc 374-389
Turpin, L., Maruejol, P., Cuney, M.: U-Pb, Rb-Sr and Sm-Nd chronology of granitic basement, hydrothermal albites and uranium mineralization (Lagoa Real, South-Bahia, Brazil) 139-147
Unger, C.P., → Windom, K.E. 390-400
Valley, J.W., → Morrison, J. 97-108
Varne, R., → Stolz, A.J., et al. 374-389
Velde, B., Medhioub, M.: Approach to chemical equilibrium in diagenetic chlorites 122-127
Vielzeuf, D., Holloway, J.R.: Experimental determination of the fluid-absent melting relations in the pelitic system. Consequences for crustal differentiation 257-276
Villeman, B.: Trace element evolution in the Phleorean Fields (Central Italy): fractional crystallization and selective enrichment 169-183
Wayne, D.M., Sinha, A.K.: Physical and chemical response of zircons to deformation 109-121
Wheller, G.E., → Stolz, A.J., et al. 374-389
Wilkinson, J.F.G., Hensel, H.D.: The petrology of some picrites from Mauna Loa and Kilauea volcanoes, Hawaii 326-345
Windom, K.E., Unger, C.P.: Stability of the assemblage albite plus forsterite at high temperatures and pressures with petrologic implications 390-400
Wood, B.J., → Mattioli, G.S. 148-162
Wyllie, P.J., → Johnston, A.D. 352-362

Subject-Index V

List of Locations VIII

Indexed in Current Contents/

Abstracted in Mineralogical Abstracts





Subject index

- Actinolite 4
- albite 3, 123
- albite-forsterite stability 390f.
- albite twin 447, 434
- albitite, geochronology 139f.
- alkali basalt 295f.
- , pyroxenes 81f.
- alkali enrichment, Andes volcanics 468f.
- alkali feldspar 446f.
- alkaline magmatism 277f.
- allanite 140, 280
- amphibole 3, 52, 81, 280, 378, 435
 - , solid solutions 163f.
- amphibolite 15
- anatexis 257f.
- andalusite 2
- andesite 225f., 463ff.
- ankaramite 402
- ankerite 3
- anorthosite 15, 97ff., 304
 - , Nd-Sm isotopic systematics 363ff.
 - , petrogenesis 369f.
- apatite 140
 - , carbonatites 279
 - , gneiss geochronology 316
- arc crust, subduction 482
- arc magmatism, Andes 455f.
- ash beds, illite/smectite formation 2f.
- assimilation 414f.
- angite 332, 403
- Ba, Andes volcanics 470
- banded iron formation, O isotopic exchange 491f.
- basalt 185
 - , Andes 462ff.
 - , geochemistry 295ff.
 - , subduction zones, geochemistry 72f.
- basalt lavas, fractionation 401ff.
- basanite 83, 296
- Benioff zone, Andes 455f.
- biotite 3, 140, 169, 280, 376, 435, 503
 - , biotite/garnet geothermometry 40f.
- borosilicates, metamorphic stability 512
- Bouguer Gravity anomalies, Andes 460
- britholite, carbonatites 282
- Calcite 3, 24
 - , carbonatites 285
 - , Naxos metamorphics, O-C isotopic data 29
- caldera 195
- carbonatite magmatism 277ff.
- charnockite 366
- chemical analysis
 - , alkali basalts, Massif Central 82
 - , alkali feldspar 505
 - , allanites, carbonatites 282
 - , amphibole, Batu Tara volcanics 377
 - , -, carbonatite complex 280
 - , -, metagabbro coronas 54
 - , andesite, Crater Lake 235
 - , apatite, carbonatites 281
 - , basalts, Austral Isl. 294
 - , biotite, alkaline magmas 200
 - , silicates 507
- , britholites, carbonatites 283
- , carbonatites, In'Ouzzal 286
- , chromite, picrites 330
- , clinopyroxene, alkali basalts 84
 - , -, Batu Tara volcanics 377
 - , -, carbonatite complex 280
 - , -, metagabbro coronas 54
 - , -, xenoliths 186
- , cordierite 505
- , cumulate, carbonatites 286
- , dykes, Batu Tara volcanics 378
- , feldspars, Infiernito lavas 199
- , Fe-Ti oxides, alkaline magmas 200
- , garnet, eclogites 34
- , -, metagabbro coronas 54
- , -, syenite 281
- , glass, picritic olivine inclusions 337
- , ilmenite, picrites 330
- , latite, Phleorean Fields 170
- , lavas, Batu Tara 378
 - , -, Crater Lake 227
 - , leucite, Batu Tara volcanics 377
 - , magnetite, Batu Tara volcanics 377
 - , olivine, Batu Tara volcanics 377
 - , -, metagabbro coronas 54
 - , -, picrites 328
 - , orthopyroxene, eclogite 34
 - , orthopyroxene, metagabbro coronas 54
 - , -, xenoliths 187
 - , phenocrysts, Crater Lake lavas 243
 - , picrites, Hawaii 334
 - , plagioclase, Batu Tara volcanics 377
 - , -, metagabbro coronas 54
 - , -, picrites 332
 - , pyroxenes, Infiernito lavas 198
 - , -, picrites 332
 - , rhyodacite inclusions 237
 - , rhyolite, Infiernito 196
 - , sanidine, Batu Tara volcanics 377
 - , sillimanite 505
 - , spinel, Batu Tara volcanics 377
 - , -, xenoliths 187
 - , syenite, carbonatite complex 286
 - , tholeiite, Hawaii 336
 - , Ti-magnetite, Batu Tara volcanics 377
 - , -, picrites 330
 - , trachybasalt, Phleorean Fields 176
 - , trachyte, Infiernito 196
 - , -, Phleorean Fields 170
 - , Xenoliths, Oslo Rift lavas 188
 - , zircons, shear zones 115
- chlorite 3, 24
 - , diagenetic, chemical equilibrium 122f.
- chromite 330
- clinopyroxene 51f., 169f., 184f., 195, 280, 304, 327, 375, 402, 435
 - , alkali basalts 81f.
- clinzoisite 3
- contamination, granitic-basic magma interaction 352f.
- cordierite 24, 67
- corona clinopyroxene, metagabbros 52f.
- corona formation, metagabbros 53f.
- corona orthopyroxene, metagabbros 52f.
- corona structures, anorthosite 304
- coronites, granulites 303f.
- corundum 503f.
- Cr-spinel 327
- crustal growth, Archean 312ff.
- cryptomesoperthite 446, 438
- crystal accumulation, alkaline volcanoes 387
- crystal fractionation, alkaline volcanics 384
- crystal-liquid equilibria, alkaline volcanics 385
- Dacite 225f.
- defect structures, tuff phyllosilicates 5
- differentiation, carbonatites 286
- diffusion, O in iron formation 490f.
- , Sm-Nd in garnet 309
- diffusion models, corona formation in metagabbros 49ff.
- diffusive mass transport 421
- diopside 3, 25, 169, 402
- disorder, spinels 155
- dispersion, mass transport 423
- dolomites, siliceous, phase relations 24f.
- dykes 378f.
- Eclogite, plagioclase breakdown 33f.
- endiospide 332
- equilibrium, diagenetic chlorite formation 122ff.
- Eu anomaly, volcanites, Phleorean Fields 171
- euxenite 140
- exsolution microtextures, feldspars 444f.
- Fayalite 491
- feldspars, exsolution textures 431f., 444f.
- ferrosilite 491
- flow differentiation, picrites 340
- fluid-absent melting, pelites 269f.
- fluid flow, mechanism 417
- , metamorphism 1ff.
- fluid inclusions, Oslo Rift lavas 189
- fluid rock ratios, C isotopic data in Naxos schists 30
- foildes 296
- fractional crystallization, Phleorean Fields 169f.
- fractional crystallization model, alkaline magma 197f.
- fractionation, basalts 401f.
- , models, Crater Lake lavas 247f.
- Gabbro 14, 16, 431, 444
 - , granite interactions 409f.
- garnet 4, 24, 34, 53, 67, 101, 280, 304, 503f.
- , pelite melting 260
- geochronology, anorthosites, Rogaland 365f.
- , Brazilian granites 139f.
- , granulites 305f.
- , Hercynian Fold Belt 135f.

- , ophiolites 13ff., 16f.
- geothermometry, biotite/garnet 40ff.
- , lavas 206
- Gibbs method equations, metamorphic systems 348
- glass, melting experiments 356f.
- , picrites 337
- glaucite 123
- glomerocrysts, origin 207
- gneiss 15, 131, 502f.
- , Archean crust 313ff.
- grandidierite 502ff.
- granite 140, 279
- , mafite interaction 509f.
- granodiorite 314
- granulite 131, 272, 277
- granulite facies metamorphism 97f.
- granulite terrain, P-T history 303ff.
- graphite 3
- grunerite 491
- Harzburgite 15
- hastingsite, carbonatites 285
- hedenbergite 140
- hematite 152, 493
- Hercynian orogeny 130
- Hf, zircons from shear zones 116f.
- H_2O activity, amphiboles 166f.
- hornblende 4, 491
- hydrothermal alteration, syenites 212f.
- hypersthene 64f.
- Iapetus Ocean 13
- ignimbrite 225f.
- illite/smectite interstratifications 122
- ilmenite 3, 68, 195, 503
- infiltrational mass transport 521f.
- island arc tholeiites 300
- isotopic exchange, retrograde, granulites 490f.
- K-feldspar 279
- , gneiss geochronology 316
- kinetics, isotope transport 420f.
- kink bands, olivines 329
- kornerupine 502ff.
- kyanite 24, 33f., 260
- kyanite eclogite, plagioclase breakdown 33f.
- Latite 169
- lavas, alkali basalts 81f.
- , Andes 462f.
- , Austral Isl. 295ff.
- , Crater Lake 224ff.
- , Infiernito 194f.
- leucite 375f.
- leucite basanites 374f.
- leucite tephrites 374f.
- leuconorite 366
- liquid composition, pelite melting 264
- Magma chamber zonation 208, 251
- magma contamination 408ff.
- magma interactions, experimental 352f.
- magnetite 69, 195, 280, 375, 493, 503f.
- magnetite activity, spinels 148ff.
- mangerite 304
- marble 28, 277f.
- mass-balance 424
- , anorthosites 103
- mass transport, theories 417f.
- megacrysts, pyroxenes in alkali basalts 81f.
- melting, fluid-absent, pelites 269f.
- melting experiments, albite-forsterite stability 396
- metagabbro, corona formation 49ff.
- metamorphic fluid, flow pattern 1ff.
- metamorphism, gneiss 257f.
- , granulite terrain 303f.
- , Maine 3ff.
- metapelites 24f.
- mica schists 131
- migmatite 15, 366, 491
- Mn, olivines 329
- monacite, gneiss geochronology 315f.
- muscovite 3, 123, 272
- mylonites, U-Pb data 109f.
- Nd isotopic data, granite/mafite interaction 408ff.
- , subduction-related basalts 75f.
- Nd-Sm data, Hercynian Fold Belt 132
- nephelinite 406
- Ni, olivines 329
- Ocean island basalts, trace elements 293f.
- O diffusion, granulite Fe-formations 490f.
- O isotopic data, anorthosites 101f.
- oligoclase 448
- olivine 169f., 184f., 304, 327f., 375f., 432, 435
- , coronas in metagabbros 51f.
- olivine clinopyroxenite 184f.
- olivine metagabbro, corona formation 49f.
- omphacite 34
- ophiolites, U-Pb ages 13f.
- orthoclase 140
- orthopyroxene 51f., 187, 195, 304, 332
- osumilite 272
- Partial melting, basalts 297f.
- , pelites 261f.
- , picrites 340
- Pb isotopic data, Andes volcanics 463f.
- pelites, melting relations 257f.
- pericline twin 447
- phase diagrams, metamorphic systems 346f.
- phase relations, K-alkaline volcanics 381f.
- phenocrysts, anorthosites 101
- , clinopyroxene 375, 403
- , olivine 327, 375
- , plagioclase 375
- phlogopite 285
- phonolite foidite 296
- phonolite tephrite 296
- picrite, petrology 326ff.
- plagioclase 3, 51f., 98f., 140, 169f., 195, 304, 327, 333, 375f., 403, 491, 503f.
- , eclogite 33f.
- , exsolution textures 444ff.
- , pelite melting 260
- plagiogranite 17f.
- plate tectonics, Andes 457
- postcaldera volcanism, Crater Lake 227f.
- pumice 231
- pyrite 3
- pyroxene megacrysts, alkali basalts 81f.
- pyrrhotite 3
- Quartz 3, 24, 123, 140, 272, 280, 491, 503f.
- quartz syenite 216f.
- Rb-Sr data, anorthosites 366
- , Brazilian granulites 139f.
- , granitoids 133
- , syenites 215f.
- REE, Andes volcanics 473f.
- , carbonatite minerals 283f.
- rhodocroite 225f.
- rhyolite 195
- Samarskite 140
- sanidine 195, 448
- sapphirine 272
- sapphirine-spinel phase relations 64ff.
- scoriae 235
- serpentinite 15
- shear zones, zircon U-Pb data 110f.
- siderite 493
- sidewall crystallization, gabbro-syenite contact 439f.
- sillimanite 260, 503f.
- Sm-Nd data, Brazilian granites 139f.
- , coronites in granulites 305f.
- Sm-Nd geochronology, anorthosites 365f.
- spheire 280
- spinel 51, 64f., 148f., 304, 329, 503f.
- , pelite melting 260
- , thermodynamics 91f.
- Sr-Nd data, Andes volcanics 463f.
- stable isotope transport theory 417f.
- staurolite 2
- steady state equations, coronas in metababbros 58
- subduction 72f.
- subsolidus equilibria, pelites 257f.
- subsolidus experiments, albite-forsterite stability 394f.
- substitutions, carbonatite minerals 281f.
- syenite 278, 431, 444
- , hydrothermal alteration 212f.
- syenodiorite 431
- symplectite 508
- , coronas in metagabbros 52f.
- synthesis, spinels 149
- Talc, siliceous dolomites 24f.
- tephrites 296
- thermodynamic projection, metamorphic systems 346f.
- thermodynamics, corona formation in metagabbros 49ff.
- , spinels 155
- , Zn-Cr spinels 91f.
- tholeiite 336, 401f.
- titaniite, gneiss geochronology 315f.
- tonalite 4f., 313
- tourmaline 502f.
- trace elements, alkali basalts 82
- , Andes volcanics 470ff.
- , basalts 296f.
- , Batu Tara volcanics 379f.

- , carbonatite minerals 281f.
- , Crater Lake lavas 236f.
- , ocean island basalts 293f.
- , picrites 337
- , subduction-related basalts 72f.
- , volcanites, Phleorean Fields 169f.
- trachybasalt 169, 402
- trachyphonolite 169
- transport, stable isotopes 417ff.
- tremolite, phase equilibria 163f.
- , siliceous dolomites 24f.
- trondhjemite 4f., 18
- tuff 226f.
- U-Pb data, Archean gneiss 315f.
- , Brazilian granites 139f.
- , mylonites 109ff.
- , ophiolite complex 17f.
- upper mantle, O fugacity
- Volcanism, Crater Lake 224ff.
- , K-rich alkaline 374f.
- Wollastonite 288
- Xenoliths, Oslo Rift 184f.
- Zircon 142, 280
- , gneiss geochronology 315f.
- , mylonites, U-Pb data 109ff.
- zoning, feldspar 441, 444f.
- Zr, Andes volcanics 478

List of locations

- Abitibi, Ontario 313
- Abu Khrug Complex, Egypt 213
- Adirondack Mts., N. York 99
- Ahaggar, Algeria 278
- Ana-Sira Massif, Norway 364
- Andes, Chile 456
- Ascutney Mt. Complex, Vermont 409
- Austral Isl., Pacific 293
- Batu Tara, Sunda Arc 375
- Bergen, Norway 304
- Bjerkreim-Sokndal, Norway 364
- Bohemian Massif 130
- Boutaresse, Massif Central 89
- Casimiro, Andes 456
- Cedar Lake, Ontario 313
- Cerro Alto, Andes 456
- Chaîne des Puys, Massif Central 88
- Cornwall 130
- Crater Lake, Oregon 226
- Damaraland, Namibia 24
- Daniels Lake, Ontario 313
- Egersund-Ogna Massif, Norway 364
- Eia-Rekefjord Intrusion, Norway 364
- Farsund, Rogaland 364
- Gananoque, Ontario 504
- Gaupås, Norway 304
- Glenelg, Scotland 33
- Gullfjellet, Karmoy 14
- Håland Massif, Norway 364
- Hallowell Pluton, Maine 2
- Harz, Germany 130
- Heilleren Massif, Norway 364
- Holsnøy, Norway 304
- Ihouhaouene, Ahaggar 278
- Infiernito Caldera, Texas 195
- In'Ouzzal, Ahaggar 278
- Jan, Mayen 402
- Karmoy, Norway 14
- Kauai, Hawaii 406
- Kedora, Ontario 313
- Kilauea, Hawaii 326
- Klokken, Greenland 431, 444
- Lac Seul, Ontario 41
- Lagoa Real Complex, Brazil 140
- Leka, Norway 15
- Maine, USA 2
- Maipo, Andes 456
- Marais de Limagne, Massif Central 88
- Marcy Massif, Adirondacks 99
- Marmolejo, Andes 456
- Marotiri, Austral Isl. 293
- Marquesas Isl. Pacific 293
- Massif Central, France 81, 130
- Mauna Loa, Hawaii 326
- Mont Briancon, Massif Central 88
- Montgros, Massif Central 89
- Mount Ascutney, Vermont 409
- Mount Mazama, Oregon 226
- Naxos, Greece 29
- Nazca Plate 457
- Nevado de Longaví 556
- Nevados de Chillán 456
- Odenwald, Germany 130
- Oslo Rift, Norway 184
- Palomo, Andes 456
- Phleorean Fields, Italy 169f.
- Port Kent-Westport, N. York 100
- Puy du Roi, Massif Central 88
- Raivavae, Austral Isl. 293
- Rapa, Austral Isl. 293
- Rheinisches Schiefergebirge, Germany 130
- Rimatara, Austral Isl. 293
- Rogaland, Norway 364
- Rurutu, Austral Isl. 293
- Sangrenge, Sunda Arc 375
- San Pedro Pelliado, Andes 456
- Sao Francisco Crafon, Brazil 140
- Schwarzwald, Germany 130
- Sharp Peak, Crater Lake 226
- Society Isl., Pacific 293
- Sordo Lucas, Andes 456
- Soromundi, Sunda Arc 375
- Spessart, Germany 130
- Stavfjorden District, Norway 16
- St. Regis, Adirondacks, N. York 99
- Sunda Arc, Indonesia 375
- Superior Prov., Ontario 40
- Tarreyres, Massif Central 89
- Three Mile Pond Pluton, Maine 2
- Togus Pluton, Maine 2
- Tuamoto Isl., Pacific 293
- Tubuai, Austral Isl. 293
- Tupungatito, Andes 456
- Tupungato, Andes 456
- Vosges, France 130
- Westport, Ontario 504
- Wind River Range, Wyoming 491
- Winnipeg River, Ontario 313